

Dominant factors affecting erosion-corrosion resistance of aluminum–brass pipelines

T. Liptakova*, V. Zatkalikova*, A. Alaskari** and M. Malcho***

*Department of Material Engineering, Faculty of Mechanical Engineering, University of Zilina, Zilina, Slovak Republic

**Department of Manufacturing Engineering Technology, College of Technological Studies, PAAET, Shuwaikh, Kuwait.

***Department of Energetic Technology, Faculty of Mechanical Engineering, University of Zilina, Zilina, Slovak Republic

**Corresponding Author: aalaskari@gmail.com

ABSTRACT

The degradation processes of aluminum–brass (CuZn20Al2As) alloy pipes were investigated in stagnant and flowing environments of various compositions. The experimental materials were randomly chosen aluminum–brass pipes, defined by the same standard but with slightly different chemical compositions, microstructures, and surface conditions. These characteristics have a significant influence on corrosion and erosion-corrosion degradation. To determine the most-dominant parameters affecting the resistance to degradation under different operating conditions, several corrosion and erosion-corrosion tests were performed. The corrosion resistance was evaluated by potentiodynamic and exposure tests using a designed and constructed pipeline system to simulate the operation conditions of pipes in the cooling system of a power plant and allow three different flow rates at the same time. Thus, it was possible to evaluate the influence of erosion corrosion on the same liquids at different flow rates while keeping all other experimental conditions identical. The erosion-corrosion behaviors of the tested materials were evaluated in an original experimental device, and the obtained results made it possible to evaluate the degradation processes of the material characteristics under stagnant and flowing conditions.

Keywords: Aluminum–brass; corrosion; erosion; flow; pipes.

INTRODUCTION

Aluminum–brass alloys are used in the cooling systems of power plants owing to their good heat conductivity, workability, and corrosion resistance. Various operating conditions cause material degradation that influences the properties, reliability, and working life of all devices in the system, thereby affecting the safety and economy of these devices (Syrret *et al.*, 2006; Callister & Rethwish, 2010).

Aluminum–brass alloys have been the main interest of researchers for the past few years owing to their great mechanical properties and outstanding corrosion, erosion, and wear resistances. The chemical composition, microstructure, and properties of complicated oxide systems on the surface are influenced by many factors, such as the material's chemical composition, passive layer formation, heat treatment process, and surface treatments, which have been considered by many authors (Sarver *et al.*, 2009; Davis, 1993; Karpavalli & Balasubramanian, 2007; Powell & Webster, 2012; Castle & Epler, 1976; Kato *et al.*, 1980; Alfantazi *et al.*, 2009; Chen *et al.*, 2009; Mohamednejad *et al.*, 2014; Pomenic, 2013). According to Mohamednejad *et al.* (2014) and Pomenic (2013), the cold drawing of aluminum–brass alloy increases general corrosion attacks in comparison with annealed brass. Annealing conditions improve not only the corrosion resistance and surface behaviors but also the mechanical properties (Ozgowicz *et al.*, 2010). Surface roughness is also an important parameter, because it affects the mechanism and kinetics of the corrosion process (Alaskari *et al.*, 2014; Liptakova *et al.*, 2016), flow condition, creation of deposits, crack initiation, turbulent effect of flow liquid, and instability in viscous layers (Soukup, 1995; Thulukkanam, 2013). Higher annealing temperatures of intermediate recrystallization during the tube drawing process cause not only grain growth but also a higher homogeneity of atom distribution of alloying elements in the solid solution. Grain size and homogeneity

influence not only the mechanical properties but also the erosion-corrosion properties, because grain boundaries are sensitive to corrosion attack (Wang & Li, 2001).

The corrosion behavior of aluminum–brass alloys also depends on operating conditions such as temperature, corrosivity of working liquid, and flow rate, which have been previously reported by various research groups (King, 2002; Tao & Li, 2007; Oishi *et al.*, 1982; Feron, 2007; Namboodhiri *et al.*, 1982). Surface changes in a flowing corrosion medium decrease resistance to corrosion attacks, and the result is a high combined effect of corrosion and mechanical damage (Watson *et al.*, 1995; Landolt *et al.*, 2001), which implies a higher material loss at the surface (Tao & Li, 2007). The combined effect of both the factors depends on the structure and corrosiveness of the environment and electrode potential in a given medium. This problem has been a focus area for many scientists, but the contribution of corrosion and erosion wear was not precisely quantified (Noel & Ball, 1983; Abd-El-Kader & El-Raghy, 1986; Tao & Li, 2006). Aluminum–brass pipes are mostly used for transporting liquids and are therefore exposed to chemicals and mechanical forces. Hydraulic shear forces in rapidly flowing media can damage protective oxide films, and this eventually leads to corrosion-erosion damage. Tube materials are rated according to the hydraulic forces that they can withstand. Thus, ratings are expressed in terms of the shear stress or the maximum or critical flow velocities that the pipes can tolerate without damage. Some studies (Sick, 1972) recommended flow rates of 1–2 m/s for copper, and they vary depending on their mechanical properties. Handbook data and other researchers (Syrret *et al.*, 2006; Thulukkanam, 2013; Kozubkova & Carnogurska, 2006; Stack *et al.*, 1997; Syrett & Wing, 1980) indicated that the critical shear stress of aluminum–brass alloy should not exceed 19.2 N/m² for flow velocities ranging from 0.8–2 m/s to prevent damage to the oxide layer.

The objective of the present work is to determine the dominant and controlling factors affecting the susceptibility of four aluminum–brass alloys, with similar chemical compositions, to degradation. For this purpose, various corrosion and corrosion-erosion tests have been done. The corrosion and erosion-corrosion properties were evaluated considering the effects of several factors such as microstructure and surface oxidizing surface, on aluminum–brass alloys simultaneously. In this study, four aluminum–brass samples (coded M1–M4) were selected with different standard affiliations (EN 12451, ASTM B111, and DIN 1785) but with the same chemical compositions and accepted quality. Each sample was exposed to different working hours in the cooling system but with identical working conditions. The corrosion rates were determined using electrochemical corrosion and exposure tests in both 3.5% NaCl solution and the original treated cooling water used in the cooling systems of power plants. Erosion-corrosion properties were investigated in the designed and constructed pipeline system using the two solutions. This not only saved a lot of time but also made it possible to test all four specimens simultaneously at three flow rates.

MATERIAL AND EXPERIMENTAL SETUPS

The chemical compositions of the experimental materials were determined by spectral analyses on SPECTROMAX, which satisfied the EN 12451, ASTM B111, and DIN 1785 standards (Table 1).

Table 1. Chemical compositions of the experimental aluminum–brass materials.

Content of elements [wt.%]									
Sp.	Zn	Al	As	Sn	Mn	Pb	Fe	Ni	Cu
M1	22.49	2.11	0.018	0.004	0.001	0.01	0.02	0.001	75.21
M2	23.43	2.06	0.020	0.022	0.005	0.016	0.05	0.049	74.08
M3	22.65	2.10	0.018	0.002	0.001	0.005	0.08	0.001	75.07
M4	22.07	2.06	0.025	0.014	0.008	0.01	0.02	0.135	75.47

As shown in the table, there are no major differences among the compositions of the four samples that can affect mechanical and corrosion properties. Aluminum, arsenic, manganese, and iron contents can negatively affect alloy

properties (Sarver *et al.*, 2009, Davis, 1993). The M2 specimen has a slightly higher Sn content than other samples, which may influence the behavior of the alloy. The internal surfaces of the M1, M2, and M3 specimens were covered with gray–brown passive layers, while M4 was pickled (15 vol.% H₂SO₄ + 85 vol.% H₂O at room temperature), and no oxidizing layers were visually observed.

The microstructures of all the aluminum–brass pipes (shown in Figure 1) were obtained using a solid solution of alloying elements (α). The scanning electron microscopy (SEM) analysis showed that all the tested specimens were single-phase alloys without the presence of any aggregates, and the precipitation processes were observed. The average grain size of each sample was measured, and the values are listed in Table 2. The grain sizes of all four samples were found to be different. This can be a result of different heat treatments employed for each sample. The grain size inhomogeneity was particularly observed for M1 and M3 specimens, where the numbers of grains with sizes smaller than 10 μm were much higher in comparison to the M2 and M4 specimens. The small grains created some clumps in the microstructure, as depicted in Figure 1. The most homogeneous microstructure was observed for M2. The effect of grain size can also be clearly observed in terms of the viability of the average hardness of each sample listed in Table 2.

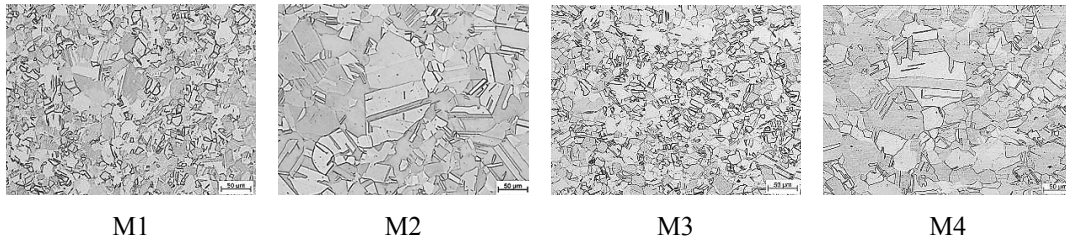


Figure 1. Microstructure of the aluminum–brass in cross section samples (200 x).

Table 2. Average grain sizes and hardness of the aluminum–brass samples.

	M1	M2	M3	M4
Avg. grain size (μm)	26	42	24	38
Avg. Hardness (HV)	88.6	75	90.6	78.4

As shown in the SEM images in Figure 2, pores, cracks, and pits were observed on the surfaces of all the specimens. Straight lines along the pipe were visible on the surface of the M3 specimen and its chemical composition, measured by energy-dispersive X-ray spectroscopy (EDX), confirmed the differences between all samples, in terms of oxygen content; these observations are in agreement with a previous study (Liptakova *et al.*, 2015). This implies that various oxidation products were produced during the manufacturing of pipes by the passivating operation. In the case of the M4 specimen, which was pickled, no dark-colored oxidizing products were observed on the surface.

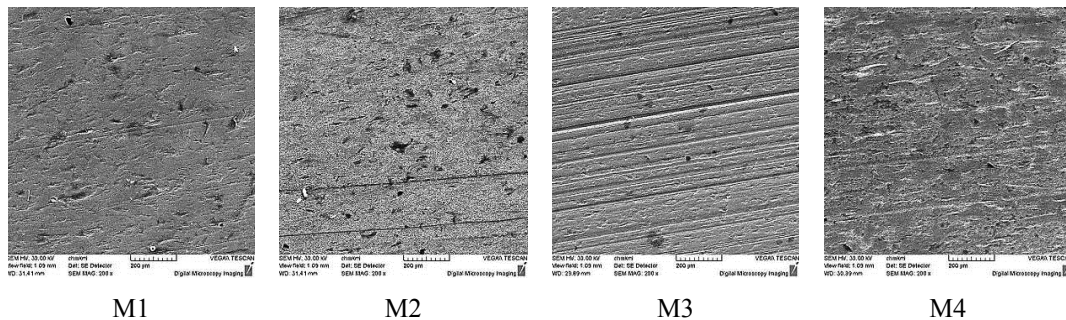


Figure 2. Internal surface of the aluminum–brass samples by SEM.

Roughness for all the samples was measured in a longitudinal direction. The mean values of the profile representative parameters (R_a -arithmetical mean deviation, R_z -maximum height, and R_{sk} -skewness) were determined following the EN ISO 4287 standard (EN ISO-4287, 1999), and the values are listed in Table 4. The M4 specimen exhibited the highest roughness of the internal surfaces among all the samples.

Table 3. Internal surface roughness parameters of the tested pipes.

Sample/conditions	R_a (μm)	R_z (μm)	R_{sk} (μm)
M1 original	0.59	6.02	-1.67
M2 original	0.57	6.09	-1.45
M3 original	0.77	5.54	-0.60
M4 original	1.29	11.50	-0.65

RESULTS AND DISCUSSION

Corrosion tests

The corrosion resistance of the tested specimens was studied in a 3.5% NaCl solution (pH 7.5; $\kappa = 54.7$ mS/cm) and in the original cooling treated water (pH = 8.4; $\kappa = 1.1$ mS/cm) at a temperature of $23 \text{ }^\circ\text{C} \pm 2 \text{ }^\circ\text{C}$. An aluminum–brass alloy was used as the working electrode with an area of 1 cm^2 , and calomel and platinum were used as the reference and counter electrodes, respectively. The corrosion test was performed using a computer-controlled potentiostat/galvanostat VSP with a setting delay of 10 min, with the potential varying between -200 and +400 mV vs. E_{oc} , and a scan rate of 1 mV/s. The potentiodynamic corrosion characteristics (E_{cor} : corrosion potential; i_{cor} : current density) of the aluminum–brass specimens in 3.5% NaCl solution and treated water are listed in Table 4. The influence of surface treatment was evident, but the effect of microstructure and chemical composition was not observed when comparing the values of E_{corr} and i_{corr} . The characteristics of the corrosion attack after the potentiodynamic tests are shown in Figure 3. The corrosion attack was most evident in the M4 sample. The corrosion rates obtained by potentiodynamic and exposure tests in similar environments are listed in Tables 4 and 5, respectively. It is interesting that passive layers were affected (on the basis of potentiodynamic test), but this effect was not marked on the M4 specimen after exposure tests in both environments. The differences in results are caused by different mechanisms and control steps of corrosion processes in the potentiodynamic test, as well as the long-lasting exposure tests.

Table 4. Results of potentiodynamic tests in 3.5% NaCl solution and treated water performed on original surfaces.

Specimen	3.5% NaCl solution		Treated water	
	E_{cor} [mV]	i_{cor} [$\mu\text{A}/\text{cm}^2$]	E_{cor} [mV]	i_{cor} [$\mu\text{A}/\text{cm}^2$]
M1	-195	0.194	-64	0.046
M2	-197	0.332	-82	0.035
M3	-200	0.285	-62	0.042
M4	-237	1.816	-104	0.088

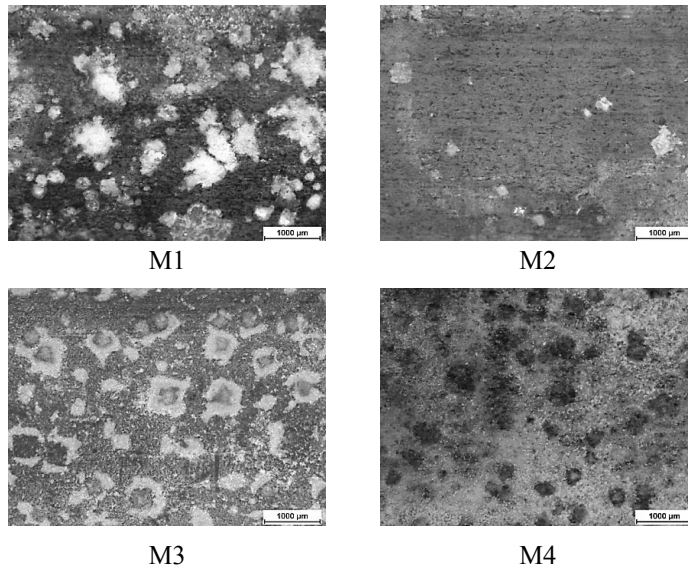


Figure 3. Corrosion attack on aluminum brass specimens after potentiodynamic test in 3.5% NaCl solution.

Table 5. Corrosion rates based on exposure tests.

Specimen	3.5% NaCl solution	Treated water
	v_{cor} [g/m ²]	v_{cor} [g/m ²]
M1	4.09	1.21
M2	5.71	0.9
M3	5.12	1.04
M4	4.07	1.08

To determine the effect of the surface state, potentiodynamic tests were performed in the same manner as done previously, but with ground surfaces (abrasive paper, grit size 500, and subsequently 1200) of all samples (Table 6). The results of the potentiodynamic tests shown in Figures 4 and 5 demonstrate that passive layers provide effective protection against corrosion attack from the thermodynamic (corrosion potential) and kinetic point of view (corrosion rate) in both corrosive environments. In the less corrosive environment, corrosion resistances of the specimens with identically treated surfaces (ground) were similar (Figure 5). In the more corrosive NaCl solution, only slight differences among the experimental specimens were observed (Figure 4).

Table 6. Results of potentiodynamic tests in 3.5% NaCl solution and treated water carried out on ground surfaces.

Specimen	3.5% NaCl solution		Treated water	
	E_{cor} [mV]	i_{cor} [μA/cm ²]	E_{cor} [mV]	i_{cor} [μA/cm ²]
M1	-229	9.639	-104	0.842
M2	-230	5.811	-95	0.872
M3	-221	11.733	-97	0.659
M4	-243	4.932	-102	0.883

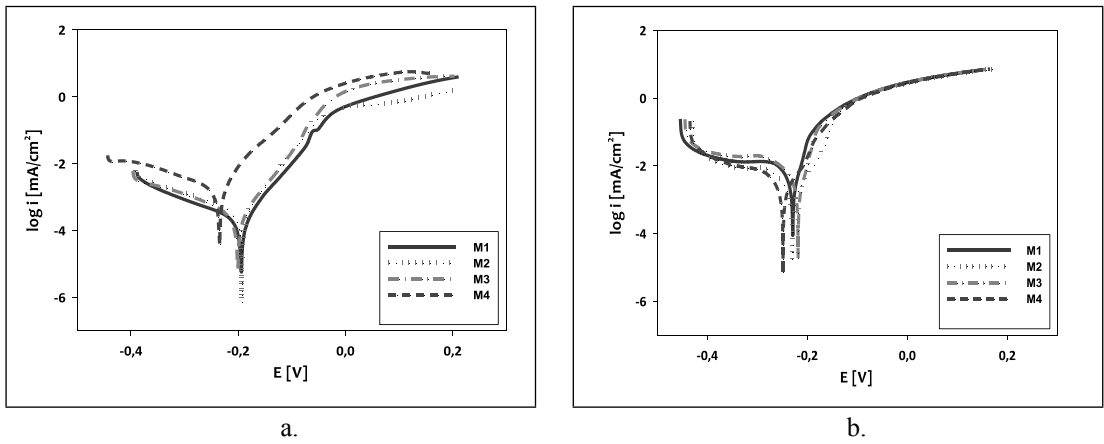


Figure 4. Comparison of potentiodynamic curves in NaCl solution (a) without ground surfaces and (b) with ground surfaces.

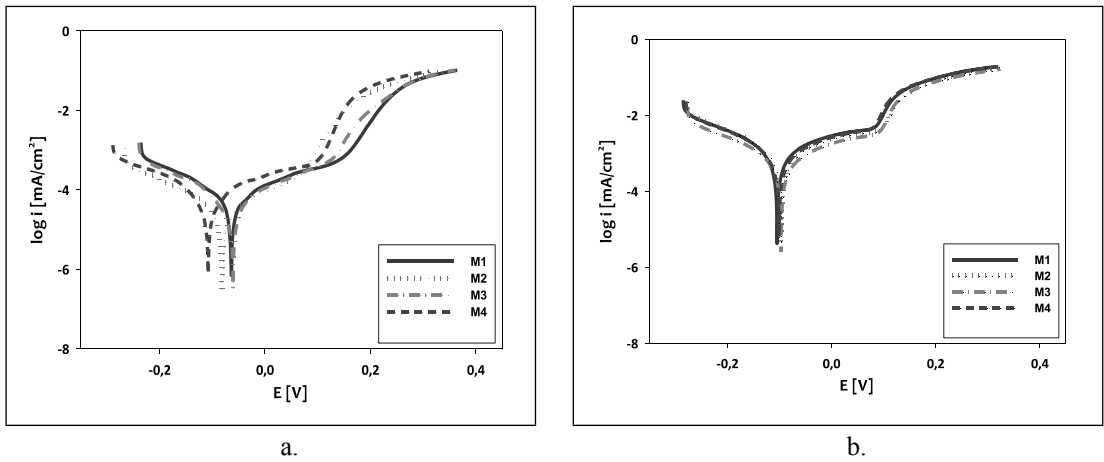


Figure 5. Comparison of potentiodynamic curves in treated water (a) without ground surfaces and (b) with ground surfaces.

Erosion-corrosion tests

A pipeline system was designed and constructed to run for 3.5 months at three different flow velocities (0.7, 1.4, and 2.8 m/s). All the aluminum–brass tubes were tested at the same time by using the pipeline system to ensure identical conditions when operated at various flow velocities. This was important for the comparison of the erosion-corrosion resistance of the tested pipes. The experiments were conducted in both environments (treated water and 3.5% NaCl solution) and lasted 2520 h in stagnant and flowing conditions. The pipeline system was operated for 8 h per day at a temperature of $43\text{ }^{\circ}\text{C} \pm 3\text{ }^{\circ}\text{C}$, and then it was kept stagnant for 16 h per day at a temperature of $22\text{ }^{\circ}\text{C} \pm 3\text{ }^{\circ}\text{C}$. The pipeline designs are shown in Figure 6. The input flow was calculated using the computational fluid dynamics method in ANSYS – FLUENT. The cross sections of the pipeline system, flow speed, calculated Reynolds numbers, and shear stresses are listed in Table 7.

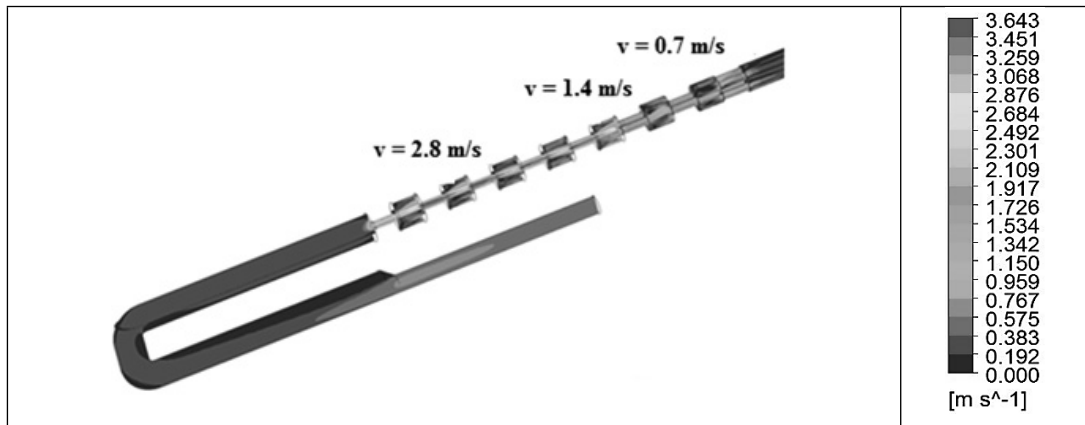


Figure 6. Operating part of the device with defined flow velocities.

Table 7. Flowing velocities, Reynolds number, and shear stresses in different sections of the experimental constructed pipeline system (for 3.5 % NaCl solution and treated water).

Sections	Flowing rates	Reynolds number values	Shear stress on the inner pipe wall Pa
	$V = 2.8$ [m/s] (NaCl) $V = 2.8$ [m/s] (water)	$Re = 82\ 232$ (NaCl) $Re = 85\ 106$ (treated water)	$\tau_0 = 21.05$ (NaCl) $\tau_0 = 20.42$ (treated water)
	$V = 1.4$ [m/s] (NaCl) $V = 1.4$ [m/s] (water)	$Re = 41\ 116$ (NaCl) $Re = 42\ 553$ (treated water)	$\tau_0 = 5.71$ (NaCl) $\tau_0 = 5.54$ (treated water)
	$V = 0.7$ [m/s] (NaCl) $V = 0.7$ [m/s] (water)	$Re = 20\ 558$ (NaCl) $Re = 21\ 277$ (treated water)	$\tau_0 = 1.44$ (NaCl) $\tau_0 = 1.40$ (treated water)

The M1, M2, M3, and M4 specimens were also exposed for the same time in identical solutions (treated water and 3.5% NaCl solution) and temperatures, but without flowing. The evaluation was performed by means of weight losses per unit area and microscopic and SEM analyses. Furthermore, all weight losses per exposed area of the experimental aluminum–brass alloys after 2520 h in stagnant and flow conditions in both environments were obtained, and the results are shown in Figure 7.

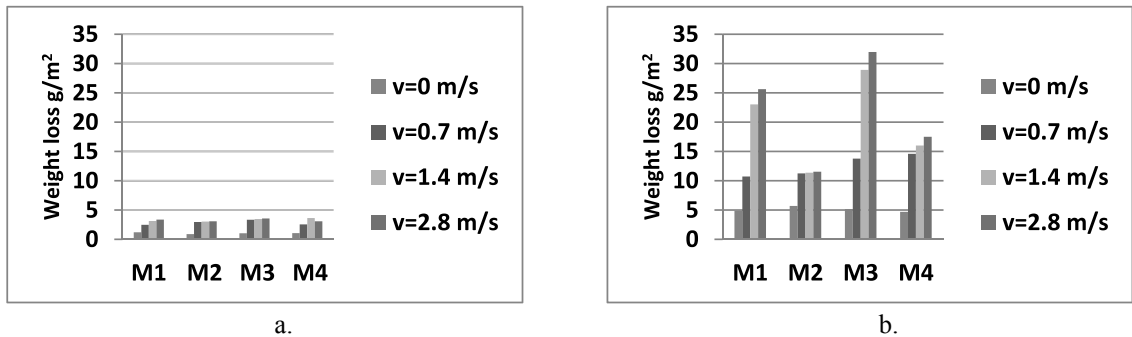
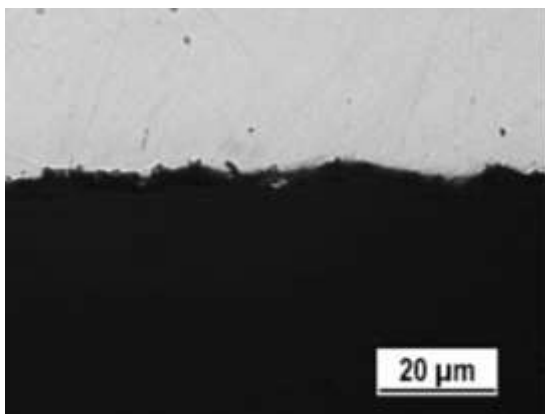


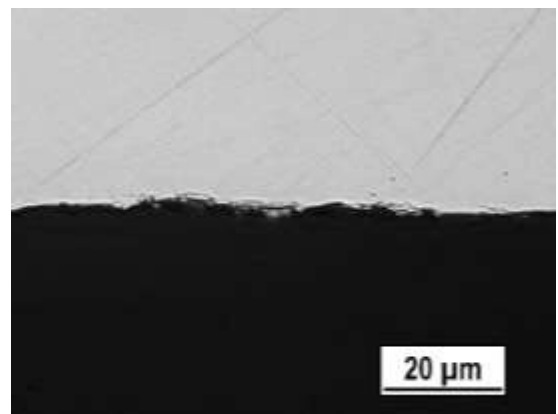
Figure 7. Weight losses of tested aluminum–brass samples at different flow rates for (a) treated water and (b) 3.5% NaCl solution.

The differences in weight loss in treated water for a stagnant condition are too small (0.9–1.2 g/m²) and can be negligible. As the flow rate increases, the weight losses increase as well (2.48–3.80 g/m²). However, when the designed pipeline system is used under stagnant conditions, higher weight losses (4.9–5.7 g/m²) occur in the NaCl solution compared with those in treated water. This agrees with the data obtained from exposure tests listed in Table 5. Under flowing conditions, the weight losses for all samples are high (11–32 g/m²) in NaCl solution, especially as the flow rate increases. The inner surfaces of all samples at a flow rate of 2.8 m/s in 3.5% NaCl solution, shown in Figure 8, show rougher surface conditions for samples M1 and M3 than the other samples, indicating higher weight losses.

The M2 and M4 samples exhibited the greatest corrosion resistance at all flow rates. This is because of the homogeneous microstructure, because of which increasing flow rates have a negligible effect on material removal. The corrosion resistance of the M1 and M3 samples was traced after the extraction of fine grains and initiation of intergranular corrosion. As Figure 9 shows, the corrosion of M1 starts at the grain boundaries, and the finer grains were extracted from the surface because of the flowing condition and thus, more weight losses were observed. The corrosion attack started during the stagnation condition, as seen on the surfaces after potentiodynamic tests in 3.5% NaCl solution in Figure 3, and weight losses continue to increase rapidly after the flowing condition, as shown in Figures 8 and 9.



M1



M2

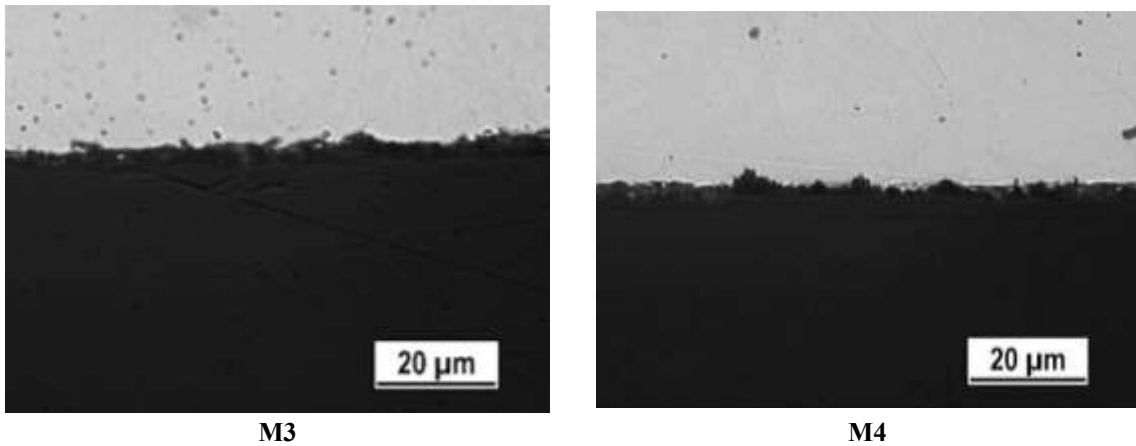


Figure 8. Inner surfaces of aluminum–brass alloys after exposing in 3.5% NaCl solution at a flow rate of 2.8 m/s.

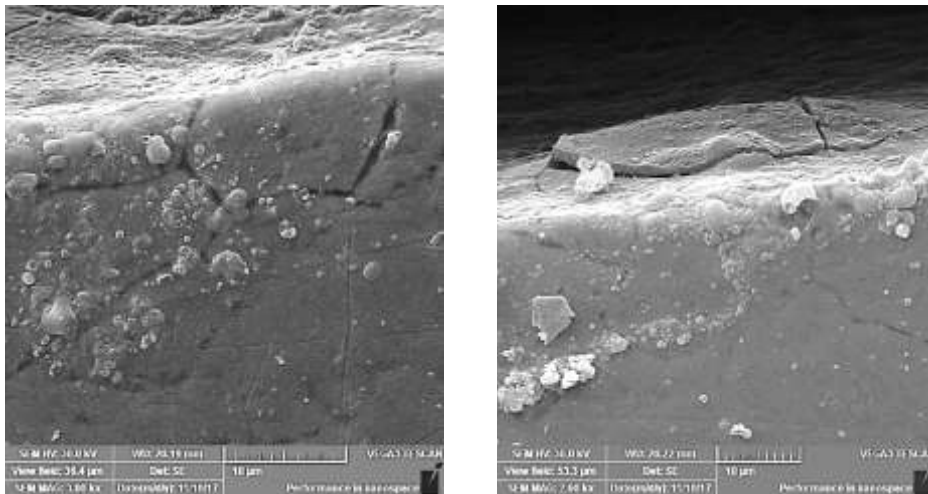


Figure 9. Details of erosion-corrosion attack on M1 specimen.

The chemical and microstructural homogeneity of the aluminum–brass tested samples were determined initially from their manufacturing history, such as casting and forming processes. Hot forming caused grain refinement and chemical homogeneity of the material by diffusion. The homogeneity and microstructure of the aluminum–brass alloy were strongly affected by the amount of forming and heat treatment parameters. Therefore, the four tested samples differed from each other, because their microstructures, mechanical and corrosion properties, and corrosion-erosion behavior were different. Grain size, microstructure homogeneity, chemical composition, and surface conditions must be inspected due to their influence on the reliability and safety of pipeline systems.

CONCLUSIONS

Based on the experimental results obtained by performing the corrosion and erosion-corrosion tests, the following can be concluded.

- Although aluminum–brass alloys with different standards have almost the same chemical compositions, different manufacturing processes affect the quality and performance of the product.
- According to electrochemical potentiodynamic tests, the corrosion resistance of the tested aluminum–brass samples

was affected by the oxidizing layers formed on the surface of the pipes. In the NaCl solution, the specimens with oxidizing layers were attacked by local corrosion, and this was evident from the corrosion rates obtained in electrochemical and exposure tests. The surface of the untreated specimen had the lowest corrosion resistance based on the electrochemical tests, but exposure tests in the same environments did not confirm this observation.

- Even though the microstructures of all the investigated aluminum–brass samples had no explicit effect on corrosion behavior, they had a substantial effect on the erosion-corrosion results.
- The flow rate and corrosivity of the flow liquid increased the erosion-corrosion attack of aluminum–brass pipes by changing the microstructure. Material weight losses at flow rates of 1.4 and 2.8 m/s with an inhomogeneous microstructure (M1 and M3) were nearly three times higher than those for the samples with a more homogeneous microstructure (M2 and M4).

ACKNOWLEDGMENT

The research is supported by the Scientific Grant Agency of Ministry of Education and the Science and Sport of Slovak Republic and Slovak Academy of Science grant KEGA 049 ZU-4/2017.

REFERENCES

- Abd-El-Kader, H. & El-Raghy, S.M. 1986.** Wear-corrosion mechanism of stainless steel in chloride media. *Corrosion Science* **26**(8): 647 – 653.
- Alaskari, A., Liptakova, T., Fajnor, P. & Halamova, M. 2014.** Mechanical treatments effect of AISI 316Ti stainless steel in chloride environment. *Journal of Engineering Research, Kuwait* **2**(3): 196-209.
- Alfantazi, A.M., Ahmed, T.M. & Tromans, D. 2009.** Corrosion behavior of copper alloys in chloride media. *Materials & Design* **30**: 2425–2430.
- Callister, W.D. & Rethwish D.G. 2010.** *Materials Science and Engineering: An Introduction*. John Wiley and Sons; 8th edition, 992.
- Castle, J. & Epler, D. 1976.** ESCA Investigation of Iron-Rich Protective Films on Aluminum Brass Condenser Tubes. *Corrosion Science* **16**: 145-157.
- Chen, J.L., Li, Z. & Zhao, Y.Y. 2009.** Corrosion characteristic of Ce Al brass in comparison with As Al brass. *Materials and Design* **30**: 1743-1751.
- Davis, D.D. 1993.** A note on dezincification of brass and inhibitive effect of elemental addition. Copper Developed Association, Inc. New York, NY, pp. 1-10.
- EN ISO-4287 - Geometrical Product Specifications (GPS).** Surface texture: Profile method - Terms, definitions and surface texture parameters, ISO 1999.
- Feron, D. 2007.** Corrosion behaviour and protection of Copper and Aluminium alloys in seawater. ISBN: 978-1-84569-241-4.
- Karpgavalli R. & Balasubmanian R. 2007.** Development of novel brasses to resist dezincification. *Corrosion Science* **49**(3): 963-979.
- Kato, C., Castle, J.E., Ateya, B.G. & Pickering, H.W. 1980.** On the mechanism of corrosion of Cu-9.4Ni-1.7Fe alloy in air saturated aqueous NaCl solution: II Composition of the protective layer. *Journal of the Electrochemical Society* **127**: 1897-1903.
- King, F. 2002.** Corrosion of copper in alkaline chloride environments. Swedish Nuclear Fuel and Waste Management Company Report, TR-02-25.
- Kozubkova, M. & Carnogurska, M. 2006.** Physical and Mathematical Modelling of Fluid Flow Dynamics in Pipe (Hydraulic Shock), *Transactions of the VSB – Technical University of Ostrava* 1/2006. Mechanical Series, Ostrava, 103-110.
- Landolt, D., Mischler, S. & Stemp, M. 2001.** Electrochemical methods in tribocorrosion: a critical appraisal. *Electrochimica Acta* **46**: 3913–3929.

- Liptakova, T., Bolzoni, F. & Trsko, L. 2016.** Specification of surface parameters effects on corrosion behavior of the AISI 316Ti in dependence on experimental methods. *Journal of Adhesion Science and Technology* **30**(21): 2329-2344.
- Liptakova, T., Lovisek, M., Hadzima, B. & Dundekova, S. 2015.** Material parameters affecting degradation processes of Al-brasses in pipe systems. *Achievements in Materials and Manufacturing Engineering* **76**(1): 27-34.
- Mohamednejad, M., Ehteshamzadeh, M. & Soroushian, M. 2014.** Effect of annealing on microstructure and corrosion performance of ADB and ALB Alloys. *Iranian Journal of Material Science and Engineering* **11**(2):1-14.
- Namoodhiri, T.K.G., Chaudhary, R.S., Prakash, B. & Agrawal, M.K. 1982.** The dezincification of brasses in concentrated ammonia. *Corrosion Science* **22**(11): 1037.
- Noel, R.E.J. & Ball, A. 1983.** On the synergistic effects of abrasion and corrosion during wear. *Wear* **87**(3): 351.
- Oishi, K., Tsuji, T. & Watanabe Y. 1982.** Proc. Int. Sym. Corrosion of copper and copper alloys in building, Ja.CDA, Tokyo.
- Ozgowicz, W., Kalinowska, E. & Grzegorzczak, B. 2010.** The microstructure and mechanical properties of the alloy CuZn30 after recrystallization annealing. *Journal of Achievements in Materials and Manufacturing Engineering* **40**(1): 15-24.
- Pomenic, L. 2006.** Electrochemical behaviour of Al-Brass in seawater. 10th International Research/Expert Conference: Trends in the development of machinery and associated technology.
- Powell, C.A. & Webster, P. 2012.** Copper alloys for marine environments, Copper development association. CDA publication No 206.
- Sarver, E., Zhang, Y. & Edwards, M. 2009.** Review of brass dezincification corrosion in portable water systems. *Corrosion review* **28**(3-4): 68-116.
- Sick, H. 1972.** Die Erosionsbeständigkeit von Kupferwerkstoffen gegenüber strömendem wasser. *Werkstoffe und Corrosion* **23**(1).
- Soukup, J. 1995.** Hydromechanics, (in Slovak) VSDS, Zilina, 1995.
- Stack, M.M., Corlett, N. & Zhou, S. 1997.** A methodology for the construction of the erosion-corrosion map in aqueous environment. *Wear* **203-204**: 474-488.
- Syrett, B.C. & Wing, S.S. 1980.** Effect of flow on corrosion of copper-nickel alloys in aerated seawater and in sulphide-polluted seawater. *Corrosion* **36**: 73-85.
- Syrret, B.C., Jonas, O. & Mancini, J.M. 2006.** Corrosion in the condensate-feedwater system. *ASM Handbook 13C*: 447-460.
- Tao, S. & Li, D.Y. 2006.** Tribological, mechanical and electrochemical properties of nanocrystal copper deposits produced by electrodeposition. *Nanotechnology* **17**: 65.
- Tao, S. & Li, D.Y. 2007.** Investigation of corrosion–wear synergistic attack on nanocrystalline Cu deposits. *Wear* **263**: 363–370.
- Thulukkanam, K. 2013.** Heat Exchanger Design Handbook, Mechanical Engineering, CRC Press, 2nd Edition.
- Wang, X.Y. & Li, D.Y. 2001.** Investigation of the synergism of wear and corrosion using an electrochemical scratch technique. *Tribology Letters* **11**(2): 117,
- Watson, S.W., Friedersdorf, F.J., Madse, B.W. & Cramer, S.D. 1995.** Methods of measuring wear corrosion synergism. *Wear* **181**(Part 2): 476.

Submitted: 23/02/2018

Revised: 10/04/2019

Accepted: 01/05/2019

العوامل المهيمنة التي تؤثر على مقاومة التآكل والتآكل المرافق بتدفق السوائل لأنابيب الألومنيوم-النحاس

تاتيانا لايتكوفافا، فيرازاتكاليكوفافا،* أمين العسكري و***ميلان مالشو

*قسم هندسة المواد، كلية الهندسة الميكانيكية، جامعة زيلينا، سلوفاكيا

**قسم تكنولوجيا هندسة التصنيع، كلية الدراسات التكنولوجية، الهيئة العامة للتعليم التطبيقي والتدريب، الكويت

***قسم تكنولوجيا الطاقة، كلية الهندسة الميكانيكية، جامعة زيلينا، سلوفاكيا

الخلاصة

تم دراسة عمليات التدهور لأنابيب من سبائك الألومنيوم-النحاس الأصفر (CuZn20Al2As) في البيئات الراكدة والمتدفقة لسبائك مختلفة. تم اختيار هذه السبائك عشوائياً لعمل التجارب لأنابيب المسبوكات التي تم تحديدها بنفس المعيار ولكن مع تركيبات كيميائية مختلفة قليلاً إما مجهرياً أو حسب ظروف السطح. هذه الفروق في الخصائص لها تأثير كبير على تدهور التآكل والتآكل المرافق بتدفق السوائل. ولتحديد أهم العوامل المؤثرة على مقاومة التدهور في ظروف التشغيل المختلفة، أجريت عدة اختبارات للتآكل والتآكل المرافق بتدفق السوائل. تم تقييم مقاومة التآكل من خلال اختبارات الجهد والتعرض الكيميائيين. كما تم تصميم وبناء خط أنابيب لمحاكاة ظروف تشغيل الأنابيب في نظام التبريد لمحطة توليد الكهرباء بحيث يسمح هذا التصميم لثلاثة معدلات تدفق مختلفة في الأنابيب في نفس الوقت. وهكذا، كان من الممكن تقييم تأثير التآكل والتآكل المرافق بتدفق السوائل داخل أنابيب اختبارها عن طريق الحفاظ على الظروف التجريبية الأخرى متطابقة. تم تقييم سلوكيات التآكل والتآكل المرافق بتدفق السوائل للمواد المختبرة في جهاز تجريبي أصلي. وسمحت لنا النتائج التي تم الحصول عليها بتقييم التأثير المشترك لبيئة التآكل والتدفق وتحديد الخصائص المادية التي لها التأثير السائد على عمليات التدهور.